Journal of Inorganic and General Chemistry
ZAAC
Zeitschrift für anorganische und allgemeine Chemie
DOI: 10.1002/zaac.201999355
ARTICLE

A Ditopic Phosphane-decorated Benzenedithiol as Scaffold for Di- and Trinuclear Complexes of Group-10 Metals and Gold

Simon H. Schlindwein,[a] Carlo Sibold,[a] Mareike Schenk,[a] Mark R. Ringenberg,[a] Christoph M. Feil,[a] Martin Nieger,[b] and Dietrich Gudat*[a]

Dedicated to Professor Dr. Manfred Scheer on the Occasion of his 65th Birthday

Abstract. The ability of 3-(diphenylphosphinomethyl)-benzene-1,2-dithiol ($pbdtH_2$) to act as ditopic ligand was probed in reactions with selected group-10-metal complexes. Reactions with $[(cod)PdCl_2]$ afforded a mixture of products identified as $[Pd(pbdtH)_2]$, $[Pd_2(\mu_2\text{-}pbdt)_2]$ and $[Pd_3(\mu_2\text{-}pbdt)_2Cl_2]$. The polynuclear complexes could be isolated after suitably adjusting the reaction conditions, and heating of a mixture in a microwave reactor effected partial conversion into a further complex $[Pd_3(\mu_2\text{-}pbdt)_3]$. Reaction of $pbdtH_2$ with $[Ni(H_2O)_6Cl_2]$ gave rise to a complex $[Ni_2(\mu_2\text{-}pbdt)_2]$, which was shown to undergo two reversible $1e^-$-reduction steps. Reaction of $[Pd(pbdtH)_2]$ with $[Au(PPh_3)Cl]$ afforded heterotrinuclear $[PdAu_2(\mu_2\text{-}pbdt)_2(PPh_3)]$. All complexes were characterized by analytical, spectroscopic and single-crystal X-ray diffraction studies. Their molecular structures confirm the ability of the $pbdt^{2-}$ unit to support simultaneous P,S- and S,S-chelating coordination to two metal centers.

Introduction

Ditopic ligands possess multiple donor functions that are arranged to provide separate binding domains for two metal centers and enable the assembly of elaborate architectures from di- and multinuclear complexes with specific molecular geometries[1] to coordination polymers and more-dimensional framework structures.[2] We have previously reported on two trifunctional ligands with mixed P,O,O- (**1**)[3] and P,S,S-donor sets (**2**)[4] that are pre-organized to create two metal binding sites (see Scheme 1). In **1**, the combination of "hard" and "soft" donor atoms inflicts different electronic preferences for both sites and enables predictable assembly of hetero-di- and multinuclear complexes through site-selective binding of "hard" and "soft" metal ions.[5] In phosphane-dithiol **2**, all three donor units are electronically more similar, and this selectivity is lost as metal species like Pd^{II} ions with a high affinity for P-donors may also readily address the sulfur atoms. Nonetheless, careful choice of the reaction conditions enabled us to access a first mononuclear complex **3**[4] featuring two mono-anionic $pbdtH^-$ ligands in P,S-chelating coordination mode (Scheme 2). We report now on an extended study of the complexation behavior of **2**, which reveals that the free ligand and its palladium complex **3** can also be used as scaffolds for the assembly of homo- or heterometallic complexes with two or three metal centers. Moreover, the synthesis of a platinum analogue of **3** is described.

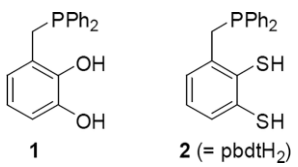

Scheme 1. Ditopic ligands **1** and **2** ($pbdtH_2$ = phosphane-benzenedithiol).

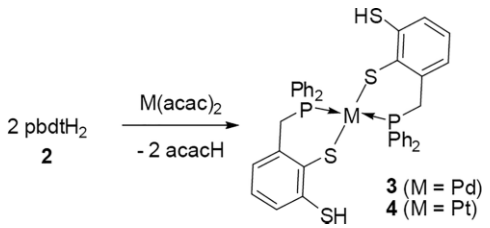

Scheme 2. Synthesis of mononuclear complexes of composition $[M(pbdtH)_2]$.

Results and Discussion

Syntheses

The reported selective outcome of the synthesis of **3** (Scheme 2) can be related to two decisive factors, viz. the use

* Prof. Dr. Dr. h.c. Dietrich Gudat
E-Mail: gudat@iac.uni-stuttgart.de
[a] Institut für Anorganische Chemie
Universität Stuttgart
Pfaffenwaldring 55
70550 Stuttgart, Germany
[b] Department of Chemistry
University of Helsinki
P.O Box 55
00014 Helsinki, Finland
Supporting information for this article is available on the WWW under **http://dx.doi.org/10.1002/zaac.201900355** or from the author.

of a tailored precursor with a predisposition to react under successive displacement of the acac⁻ units by new mono-anionic chelate ligands, and the maintenance of a metal-to-ligand ratio of 1:2 needed for exhaustive ligand exchange.[4]

We found now that the reaction of two equivalents of **2** with $[Pt(acac)_2]$ proceeds in a similar way to yield the analogous platinum complex **4** (Scheme 2), which was isolated in approx. 90 % yield and characterized by analytical and spectroscopic data and a single-crystal X-ray diffraction study. The corresponding reaction of **2** with $[Ni(acac)_2]$ was less selective and afforded, according to a ^{31}P NMR spectroscopic assay, a mixture of several newly formed species, one of which was later on identified as a 2:2 complex composed of two metal cations and two dianionic $pbdt^{2-}$ ligands (see below). The identity of the other products remains unknown, even if their ^{31}P NMR chemical shifts suggest addressing them likewise as nickel complexes. Remarkably, the 2:2 complex constituted, irrespective of the initial metal-to-ligand ratio, always the most abundant metal-containing product.

Attempts to use **3** as metallo-ligand for the assembly of homo-dinuclear complexes remained unsuccessful, but formation of a heterotrinuclear product was achieved upon reaction with two equivalents of $[(Ph_3P)AuCl]$ in the presence of triethylamine. The product formed was isolated in good yield and identified as complex **5** (Scheme 3) by analytical and spectroscopic data and a single-crystal X-ray diffraction study (see below). Observation of three distinguishable signals in the ^{31}P NMR spectrum of **5** suggests that the static solid-state structure persists in solution. The formation of **5** from **3** goes along with a shift of the palladium atom from the P,S- to the S,S-binding pocket of one of the pbdt-ligands, which underpins the exchangeability of both sites. That this isomerization was also observed in reactions of **3** with other transition metal precursors[6] suggests that the metal shift may represent a crucial step for the conversion of metalloligand **3** into more complex architectures.

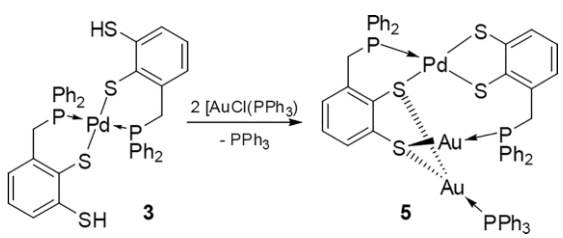

Scheme 3. Synthesis of complex **5** using complex **3** as metalloligand.

Facing the failure of a stepwise synthesis of a homo-dinuclear complex that would exploit the full capacity of the $pbdt^{2-}$ unit as ditopic ligand, we decided to approach the target compound in a single stage via self-assembly of the free phosphane-dithiol with suitable monometallic precursors. Anticipating that this strategy should benefit from using a metal-to-ligand ratio of 2:2 and a precursor with an enhanced tolerance to the binding of chelate ligands in different charge states, we investigated the reaction of equimolar amounts of **2** and $[(cod)PdCl_2]$ in the presence of a suitable acid scavenger (KO*t*Bu or a tertiary amine such as Et_3N or pyridine). The transformation proceeded readily at ambient temperature and afforded (according to a ^{31}P NMR spectroscopic assay) a mixture of three metal complexes that precipitated eventually from the reaction mixture. The main product was isolated in pure form and 48 % yield through repeated fractional recrystallization and identified by analytical and spectroscopic data and a single-crystal X-ray diffraction study as the expected 2:2 complex **6** (Scheme 4).

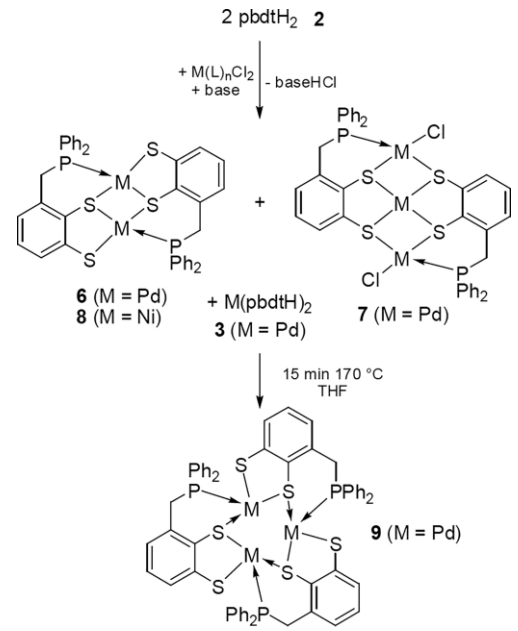

Scheme 4. Formation of homo-di- and trinuclear complexes **6**–**9** from **2** and $[(cod)PdCl_2]$ or $[Ni(H_2O)_6Cl_2]$, respectively.

Analysis of the ^{31}P NMR spectroscopic data of the crude product mixture allowed us to identify one of the minor constituents as complex **3**. Observing that this complex became the main product when $[(cod)PdCl_2]$ was treated with an excess of **2**, we presumed that its formation from a mixture containing equal molar amounts of metal ions and P,S,S-ligand is set off by formation of a metal-rich by-product. Enrichment of this species might then be feasible by using an excess of the palladium-containing reactant. In line with this hypothesis, we succeeded in producing the yet unidentified product of the original reaction with high selectivity by treating **2** with 1.5 equivalents of $[(cod)PdCl_2]$ in a solvent mixture (THF/dmso 95:5) in the presence of triethylamine as acid scavenger in a microwave reactor. The identity as complex **7** (Scheme 4) was readily established from analytical and spectroscopic data and a single-crystal X-ray diffraction study.

Reaction of **2** and an equimolar amount of $[Ni(H_2O)_6Cl_2]$ in the presence of KO*t*Bu afforded the nickel-analogue **8** of complex **6** (Scheme 4), whereas treatment with $[(cod)PtCl_2]$ produced only ill-defined, paramagnetic solids which could not be further analyzed. It should be noted that the reaction of $[Ni(H_2O)_6Cl_2]$ with two equivalents of **2** was likewise unselective and yielded a mixture in which, as in the aforementioned reaction of **2** with $[Ni(acac)_2]$, **8** was identified spectroscopically as a dominant component. Separation of the product mixture or isolation of any other component remained unfeasible.

An intriguing result was observed when the crude product of a reaction of **2** with [(cod)$PdCl_2$] in the presence of pyridine, which contained complexes **3** and **6** as the only species detectable by ^{31}P NMR spectroscopy, was dissolved in THF and heated to 170 °C in a microwave reactor. A ^{31}P NMR assay revealed that the molar fraction of **3** had been greatly reduced and a new product had formed, which serendipitously separated in crystalline form when the reaction mixture was allowed to cool down to ambient temperature. The ^{1}H and ^{31}P NMR spectroscopic data of this species bear close similarity with those of **6**, but a single-crystal X-ray diffraction study revealed the presence of a complex **9** with a trimeric rather than a dimeric structure (Scheme 4). While this species could not be generated by simple heating of solutions of pure **6**, its formation was also observed upon microwave irradiation of THF/pyridine solutions containing **7** besides **2** and/or **3**, respectively. We assume therefore that the trinuclear core is formed via base-induced condensation of **7** with excess ligand under more forcing conditions. Interestingly, this reaction requires that one of the chelate ligands on the central palladium switches from S,S- to P,S-coordination and reverses thus the isomerization observed during the formation of **5**.

Crystallographic Studies

The molecular structures of complexes **4**–**7** and **9** established from single-crystal X-ray diffraction studies are displayed in Figure 1, Figure 2, Figure 3, Figure 4, and Figure 5, and selected metric parameters are compiled in Table 1 and Table 2. A listing of crystallographic data and a plot of the molecular structure of **8** are given as Supporting Information.

Table 1. Selected distances /Å and angles /° for complexes **4**–**6**. The two columns displayed for complex **6** denote the parameters of two crystallographically independent specimens in the asymmetric unit. Numbers in parentheses denote estimated standard deviations.

	4 [a]	**5** [b]	**6** [b]	
M–P	2.282(15)	2.2652(16)	2.271(2)	2.276(2)
			2.261(2)	2.266(2)
Au–P		2.2440(17) [c]		
		2.2761(15)		
M–S_t [d]	2.3323(14)	2.2633(16)	2.319(2)	2.317(2)
		2.2861(15)	2.318(2)	2.312(2)
M–S_{br} [d]		2.3569(15)	2.333(2)	2.336(2)
			2.336(2)	2.343(2)
			2.328(2)	2.330(2)
			2.343(2)	2.349(2)
Au–S		2.4013(15) [e]		
		2.5877(15) [e]		
		2.3575(14) [f]		
M···M			3.0870(8)	3.1069(8)
Σ(X–M–Y) [g]	360.0(2)	359.7(3)	359.5(3)	359.3(3)

a) M = Pt. b) M = Pd. c) To PPh_3 ligand. d) S_t and S_{br} denote terminal and bridging S-atoms, respectively. e) To Au(1). f) To Au(2). g) Sum of all bond angles between adjacent ligands.

The crystals of **4** are isotypic with those of the previously published[4] palladium complex **3**. Complexes **6** and **8** (two modifications) crystallize as solvates with different solvent molecules (THF, CH_2Cl_2) and are not isotypic. All crystals comprise clearly separated molecular complexes which lack any specific intermolecular interactions and exhibit square-planar coordination geometry at all group-10 metal centers. The M–P distances (see Table 1 and Table 2) display no peculiarities and are close matches of the standard distance (Pd–P 2.278 ± 0.050 Å[7]) in palladium phosphane complexes. Analysis of the features of the dithiolene units reveals that all C–S bonds are essentially single bonds (C–S 1.75–1.79 Å) and the six-membered rings retain fully aromatic character, suggesting that all ligands adopt the lowest conceivable charge state and can be adequately described as benzene-dithiolates.

Table 2. Selected distances /Å and angles /° for complexes **7**–**9**. Numbers in parentheses denote estimated standard deviations.

	7 [a]	**8**·THF [b]	**8**·CH_2Cl_2 [b]	**9** [a]
M–P	2.253(2)	2.165(1)	2.1645(4)	2.2596(5)
	2.263(2)	2.176(1)	2.1791(4)	2.2583(5)
				2.2596(5)
M–S_t [c]		2.163(1)	2.1678(4)	2.2868(6)
		2.179(1)	2.1879(3)	2.2708(5)
				2.2739(5)
M–S_{br} [c]	2.300(2)	2.160(1)	2.1586(3)	2.3116(5)
	2.453(2)	2.173(1)	2.1826(3)	2.3309(5)
	2.296(2)	2.167(1)	2.1679(3)	2.3431(5)
	2.301(2)	2.175(1)	2.1846(3)	2.3469(5)
	2.270(2)			
	2.271(19")			2.3493(5)
				2.3937(5)
	2.299(2)			
	2.439(2)			
M–Cl	2.325(2)			
	2.330(2)			
M···M	3.095(1)	2.9240(5)	2.9391(3)	4.1523(3)
	3.072(1)			4.1338(3)
				3.9113(3)
Σ(X–M–Y) [d]	360.2(3)	359.0(1)	360.56(6)	361.3(1)
	356.6(3)	359.9(1)	359.93(6)	361.6(1)
	360.3(3)			360.2(1)

a) M = Pd. b) M = Ni. c) S_t and S_{br} denote terminal and bridging S-atoms, respectively. d) Sum of all bond angles between adjacent ligands.

The molecular structure of complex **4** is centrosymmetric (as imposed by crystallographic *Ci* symmetry) and characterized by a square-planar coordination arrangement at platinum and a *trans* arrangement of the two bidentate, P,S-bound ligands (Figure 1). The chelate rings adopt a boat conformation, and the bite angle of the bidentate ligand [P–Pt–S 91.88(5)°] comes close to the ideal value of 90°. Based on the observation that solution ^{1}H and ^{31}P NMR spectra of **4** display, like those of **3**,[4] a single set of signals suggests that the *trans* arrangement persists in solution, which contrasts the behavior of analogous complexes[5] derived from the P,O,O-based ligand $\mathbf{1H_2}$.

The palladium atom in heterometallic complex **5** is coordinated by one P,S- and one S,S-bound chelate ligands which exhibit essentially identical bite angles [S1B–Pd1–S2B

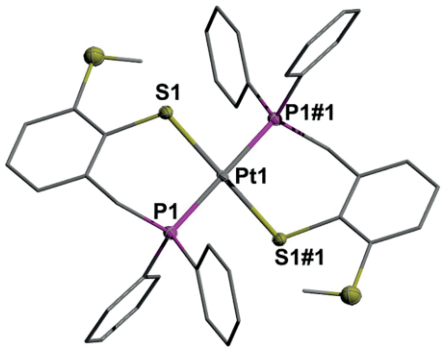

Figure 1. Representation of the molecular structure of complex **4** in the crystal. For clarity, hydrogen atoms (except those of thiol groups) and a solvent molecule (DMF) are omitted and the carbon framework of the ligands drawn using a wire model. Thermal ellipsoids are drawn at the 50 % probability level.

89.21(7)°, S1A–Pd1–P1A 88.10(6)°] and create a slightly distorted square planar PS_3 coordination sphere (Figure 2).

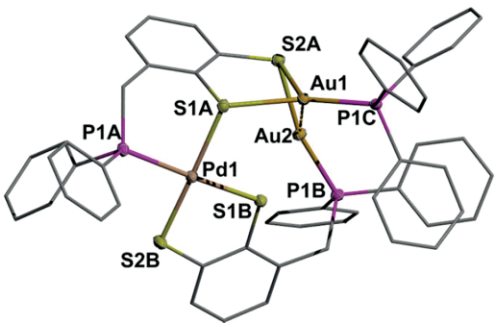

Figure 2. Representation of the molecular structure of complex **5** in the crystal. For clarity, hydrogen atoms and solvent molecules ($CHCl_3$, EtOAc) are omitted and the carbon framework of the ligands drawn using a wire model. Thermal ellipsoids are drawn at the 50 % probability level.

The remaining phosphane and thiolate moieties bind to a gold atom, which attains thus a quasi-linear [P1B–Au2–S2A 164.11(6)°] coordination sphere. The sulfur atoms of the ligand acting as a P,S-donor to palladium connect to the second gold atom, which carries an additional PPh_3. The inequality of the Au–S distances [Au1–S1A 2.4013(15) Å, Au1–S2A 2.5877(15) Å] suggests describing the metal coordination environment in terms of a dicoordinate primary unit (P1C···Au1···S1A) perturbed by a secondary interaction with a second sulfur atom (Au1···S2A). As a consequence of this perturbation, the primary unit is visibly bent [P1C–Au1–S1A 149.79(5)°] and the resulting arrangements intermediate between T- and Y-shaped. The Au1–Au2 distance of 3.0648(4) Å qualifies as a medium strong, semi-supported aurophilic interaction,[8] the presence of which may explain the preference for the observed unsymmetrical molecular structure over an alternative more symmetrical configuration.

Complexes **6**–**8** contain two (**6**, **8**, Figure 3) or three (**7**, Figure 4) group-10 metals framed by two phosphane-dithiolate ligands, each of which acts as S,S-chelating donor to one and as P,S-chelating donor to a second metal atom. The metal coordination spheres are square planar and pairwise share a common edge. The geometrical constraints of the rigid ligands prevent a coplanar arrangement and impose a folded (**6**, **8**) or half-pipe shaped (**7**) alignment with fold angles between adjacent planes of 58.6(1)° to 62.8(1)°. Even if this configuration instigates rather close metal-metal contacts [Pd···Pd 3.0718(9) to 3.0946(9) Å in **6**, **7**; Ni···Ni 2.9391(3) / 2.9240(5) Å in **8**], a closer look at the observable distortions in the local coordination spheres gives no indication for a significant attractive interaction. Altogether, the structural features of **8**, including the fold angle between the two metal coordination planes and the short intermetallic distance, match those of the known complex $[Ni_2(PPh_3)_2(\mu_2\text{-}SCH_2CH_2S)_2]$.[9]

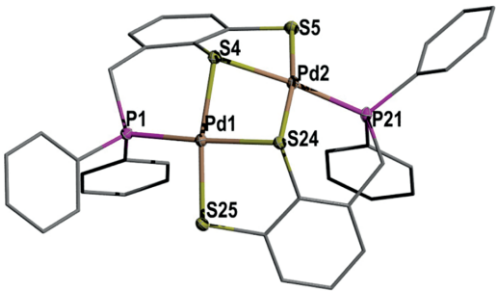

Figure 3. Representation of one of the two crystallographically independent molecules of complex **6** in the crystal. For clarity, hydrogen atoms and a solvent molecule (THF) are omitted and the carbon framework of the ligands drawn using a wire model. Thermal ellipsoids are drawn at the 50 % probability level.

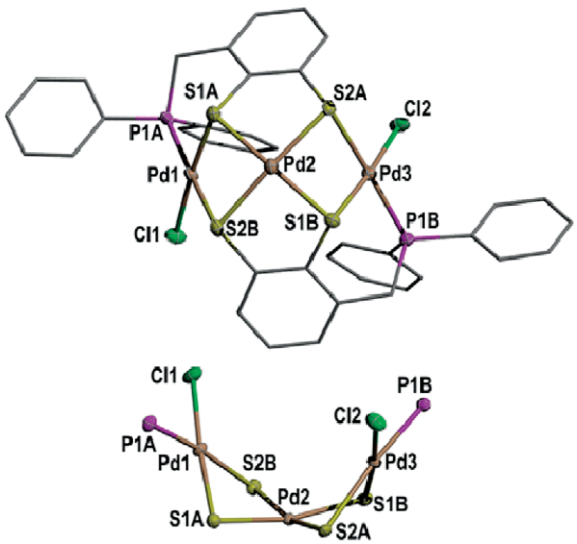

Figure 4. Molecular structure of complex **7** in the crystal (top) and reduced plot showing the trinuclear core with the first ligand sphere from a different view angle (bottom). For clarity, hydrogen atoms and a solvent molecule (DMSO) are omitted and the carbon framework of the ligands drawn using a wire model. Thermal ellipsoids are drawn at the 50 % probability level.

The central palladium atom in **7** exhibits a distinct displacement from its S_4-coordination plane away from the terminal metal centers, but it cannot be decided if this feature points to a repulsive interaction or is simply enforced by geometrical constraints or the binding preferences of the sulfur atoms. Further noteworthy features of **7** are the *transoid* orientation of

the chlorido and phosphane ligands on the terminal and the orientation of the benzenedithiolato-units on the central metal atoms, which altogether create a bowl-shaped conformation of the whole assembly. Worth mentioning is also the pronounced elongation of the Pd–S distances between the terminal metal centers and the sulfur atoms in trans-position of the phosphane ligand, which exceed all other Pd–S distances in the complexes studied by approx. 10 pm.

Complex **9** contains, like **6** and **8**, μ_2-bridging phosphanedithiolate units which act as bidentate S,S-donors to one and as P,S-donors to a second metal center. In contrast to the dimeric complexes, the coordination spheres of adjacent metal atoms share common corners rather than edges, resulting in a trinuclear framework arranged around a central Pd_3S_3 six-membered ring (Figure 5). This ring adopts a strongly distorted boat conformation in which two sulfurs are situated on one and the third one on the other side of a reference planed defined by the three metal atoms. As a consequence of this alignment, the whole assembly lacks any higher symmetry. The metal coordination environments display larger deviations from ideal planarity than in the dinuclear complexes. The ^{1}H NMR spectroscopic data indicate that the non-planar alignment of the trimetallic core is dynamically averaged in solution to give an assembly with effective C_s-symmetry.

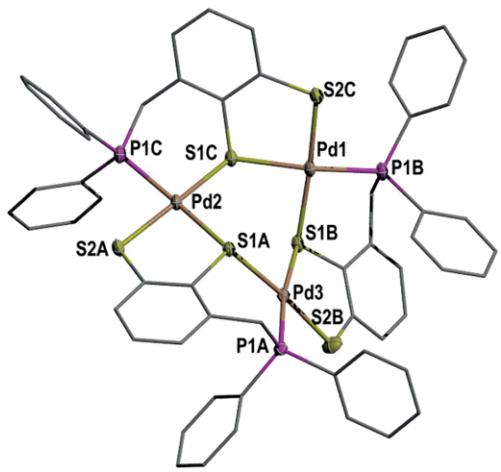

Figure 5. Representation of the molecular structure of complex **9** in the crystal. For clarity, hydrogen atoms are omitted and the carbon framework of the ligands drawn using a wire model. Thermal ellipsoids are drawn at the 50 % probability level.

Electrochemical Studies

In view of the known ability of benzodithiolene derivatives to act as redox active ligands,[10] we were also interested in studying the electron transfer behavior of the complexes prepared by cyclic voltammetry. Meaningful results were obtained for **4**, the trinuclear palladium complex **7** and the dinuclear nickel complex **8**. The cyclic voltammograms of all three complexes showed oxidation waves (at peak potentials between 0.5 to 0.8 V vs. Fc/Fc^+, Figure S3, Supporting Information) but no complementary reduction events, presumably because the oxidation products were consumed by follow-up processes. Even if attempts to identifying the reaction products by spectro-electrochemistry gave no conclusive results, these observations rule out that a reversible dithiolene redox chemistry[10] involving oxidation of the benzenedithiolato to dithiosemiquinone and dithioquinone units takes place.

The cyclic voltammogram of **7** displayed further an irreversible reduction wave at a peak potential of –1.67 V (Figure S3). Nickel complex **8** was found to undergo two reductions (Figure 6), the first of which ($E_{1/2}$ = –1.507 V vs. Fc/Fc^+) was reversible (i_{pa}/i_{pc} = –0.94) while the second one ($E_{1/2}$ = –2.054 V vs. Fc/Fc^+) was only partially reversible (i_{pa}/i_{pc} = –0.75).

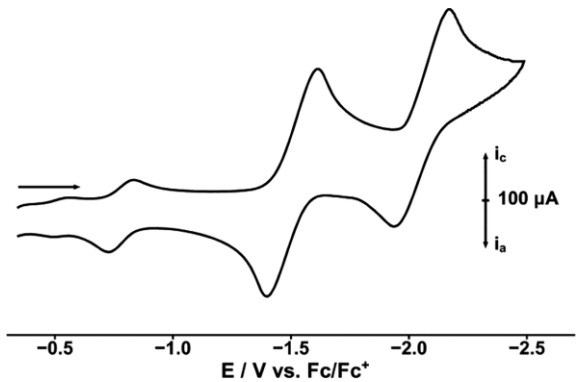

Figure 6. Cyclic voltammogram of complex **8** (conditions: scan rate 100 $mV \cdot s^{-1}$ at 25 °C in anhydrous DMF with 0.1 M $[NBu_4]PF_6$ as conducting salt, glassy carbon working electrode; ferrocene (Fc) internal standard). The initial small redox waves centered around –0.75 V arise from a paramagnetic impurity which could not be removed even after repeated recrystallization.

The separation of cathodic and anionic peak potentials (213 and 226 mV for the first and second reduction step) indicates that the electron transfer is kinetically hindered, presumably because it is associated with a change in the complex geometry. Attempts to characterize the reduction products by UV/Vis and EPR spectroelectrochemistry gave no conclusive results. However, since the pbdt-ligand in **8** adopts already its lowest charge state and further reduction seems unlikely, we assume that both reduction steps are metal-centered and can be described by the processes displayed in Scheme 5. This view was confirmed by the results of DFT calculations at the CPCM-B3LYP/def2-TZVP/J-D3BJ level on complexes $[Ni_2(pbdt)_2]^q$ (q = 1+/0/–1/–2). Energy optimization of the structure of neutral $[Ni_2(pbdt)_2]$ (**8**) resulted in metrics that are in good agreement with the experimental data and support the description as a complex containing two Ni^{II} centers and two dithiolato ligands $pbdt^{2-}$, as expected. The structural parameters of $[Ni_2(pbdt)_2]^{1+}$ differ, apart from a slight elongation of the Ni–Ni distance from 3.112 Å to 3.145 Å, not significantly from those of neutral **8**, but the calculated electron and spin density distribution (Table S2 and Figure S5, Supporting Information) suggest that the oxidation is primarily ligand-centered. Complex $[Ni_2(pbdt)_2]^{1-}$ arising from one-electron reduction of **8** contains one nickel center, which still retains similar Ni-P/S distances as in **8**, while the distances around the second nickel are noticeably elongated (Table S2, Supporting Information).

In connection with the localization of the spin density on this metal and the adjacent donor atoms (Figure S5), this feature is consistent with formation of a fully valence localized system, i.e., $Ni^{I}Ni^{II}$.

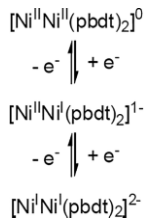

Scheme 5. Postulated mechanism of the reduction of complex **8**.

Computations on $[Ni_2(pbdt)_2]^{2-}$ allowed us to identify two configurations that can be described as singlet (S = 0) and triplet (S = 1) states of a $Ni^{I}Ni^{I}$ complex formed by antiferromagnetic or ferromagnetic coupling of the electron spins of two metal ions with formal d^9(s = ½)-electron count. The calculated spin density (Figure S6, Supporting Information) and the increase of the Ni–Ni distance (3.175 Å in ^{1}[**8**]$^{2-}$ and 3.193 Å in ^{3}[**8**]$^{2-}$ vs. 3.112 Å in neutral **8**) render the presence of a metal–metal bond in the singlet state unlikely. In regard of the very close energies (the triplet lies <0.1 kcal·mol^{-1} below the singlet state), safe assignment of the electronic ground state is currently unfeasible and requires further investigation. A reversible metal-centered reduction had previously also been established for a related mononuclear complex [Ni(dppf)(bdt)] (dppf = 1,1-bis-diphenylphosphinoferrocene, bdt = benzenedithiolate)[11] and for dinickel complexes $[Ni_2(NR\{CH_2(MeC_6H_2R')S\}_2)_2]$[12] featuring structurally related N,S,S-coordinated amino-dithiolato ligands. The redox behavior of the latter complements that of **8** in that the amine-decorated dithiolato-ligands render oxidation toward higher oxidized forms electrochemically reversible, whereas the soft phosphine donors in **8** render further reduction of an initially formed Ni^{II}/Ni^{I} complex to a Ni^{I}/Ni^{I} complex (quasi)reversible.

Conclusions

It was confirmed that phosphane-decorated benzenedithiol **2** qualifies as a compartmentalized ligand which can act as P,S-chelating ligand to one and S,S-chelating ligand to a second metal center. The lack of a pronounced site-selectivity in metal binding, which is a characteristic of the P,O,O-donor **1**,[5] favors the formation of homo-bi- and trimetallic complexes and enables easy metal-shifts between both binding pockets. The successful isolation of palladium complexes with different, even homologous (cf. **6** and **9**), molecular structures (and the failure to obtain similar results on nickel and palladium complexes) reveals that specific addressing of individual target motifs is, even in the absence of a strong site-selectivity, not per se unfeasible, but depends very subtly on the nature of the metal involved. The observations made during the synthesis of **6**–**9** indicate that reaction kinetics seems to play a very important role, but further studies are certainly needed to draw a more detailed picture. The reversible reduction of di-nickel complex **8** stimulates further studies of the redox chemistry of multinuclear pbdt complexes in order to find out how the ability of the ligands to coerce two or more metal centers into close proximity can be used to create new cooperative reactivity.

Experimental Section

All manipulations were carried out in an atmosphere of dry argon or nitrogen using standard vacuum line techniques or in glove boxes. Solvents were dried prior to use by common procedures. Microwave syntheses were carried out using an Anton Paar Monowave 400 reactor. NMR spectra were recorded at 303 K on Bruker Avance 400 (^{1}H 400.1 MHz, ^{31}P 161.9 MHz) or Avance 250 (^{1}H 250.1 MHz, ^{31}P 101.2 MHz) spectrometers. ^{1}H NMR chemical shifts were referenced to TMS using the signals of the residual protons or carbon atoms of the deuterated solvent (^{1}H: δ($CDCl_3$) = 7.24, δ(CD_2Cl_2) = 5.32, δ([D_6]DMSO) = 2.50) as secondary references. ^{31}P NMR chemical shifts were referenced using the Ξ-scale[13] with 85 % H_3PO_4 (Ξ = 40.480747 MHz, ^{31}P) as secondary reference. Coupling constants are given as absolute values. Signals of phenyl and benzene-dithiolato-substituents are denoted as Ph and bdt, respectively. (+)-ESI-mass spectra were recorded on a Bruker Daltonics MicroTOF Q instrument. Elemental analyses were obtained with an Elementar Micro Cube elemental analyzer. Cyclic voltammetry was performed on an EG&G Princeton Applied Research Potentiostat/Galvanostat Model 273A using a standard 3 electrode setup (glassy carbon working, platinum wire counter, silver wire reference), ferrocene was added during the final CV as an internal reference. The synthesis of **2** was carried out as described.[5]

Crystal Structure Determinations: Single-crystal X-ray diffraction data were collected with a Bruker AXS Nanostar C diffractometer equipped with a Kappa APEX II Duo charge-coupled device (CCD) detector and a KRYO-FLEX cooling device at 100(2) K for **6**·THF and 130(2) K for **4**·2 DMF, **5**·(CH_2Cl_2, EtOAc), **7**·DMSO, **8**·CH_2Cl_2, **8**·THF, and **9** using Mo-K_α radiation (λ = 0.71073 Å) for all samples. Crystals were selected under Paratone-N oil, mounted on nylon loops, and immediately placed in a cold stream of N_2. The structures were solved by direct methods (SHELXS)[14] and refined with a full-matrix least-squares scheme on F^2 (SHELXL[15]). Numerical or semi-empirical absorption corrections from equivalents were applied for all structures. Non-hydrogen atoms were refined anisotropically (disordered atoms isotropically). One disordered solvent molecule (ethyl acetate) in the crystal structure **5**·CH_2Cl_2·EtOAc and two disordered solvent molecules (CH_2Cl_2) in the crystal structure of **9**·2CH_2Cl_2 were removed using the SQUEEZE routine in the program Platon.[16] **6**·THF was refined as an inversion twin, and for **8**·CH_2Cl_2 an extinction correction was applied.

Crystallographic data (excluding structure factors) for the structures in this paper have been deposited with the Cambridge Crystallographic Data Centre, CCDC, 12 Union Road, Cambridge CB21EZ, UK. Copies of the data can be obtained free of charge on quoting the depository numbers CCDC-1972321 (**4**·2DMF), CCDC-1972325 (**5**·CH_2Cl_2, EtOAc), CCDC-1972324 (**6**·THF), CCDC-1972339 (**7**·DMSO), CCDC-1972322 (**8**·CH_2Cl_2), CCDC-1972323 (**8**·THF), and CCDC-1972326 (**9**·2CH_2Cl_2) (Fax: +44-1223-336-033; E-Mail: deposit@ccdc.cam.ac.uk, http://www.ccdc.cam.ac.uk)

Complex 4: A solution of $Pt(acac)_2$ (45 mg, 0.15 mmol) and **2** (100 mg, 0.30 mmol) in THF (10 mL) was agitated in an ultrasound

bath until a yellow solid precipitated. The reaction mixture was stirred overnight. The precipitate formed was collected by filtration, washed with THF (3 × 10 mL) and dried in vacuo. Yield 104 mg (89 %). **^{1}H NMR** ([D$_6$]DMSO): δ = 4.04 (br., $^3J_{H,^{195}Pt}$ = 46 Hz, 4 H, CH$_2$), 5.16 (s, 2 H, SH), 6.89 (t, $^3J_{HH}$ = 7.6 Hz, 2 H, bdt), 7.07 (d, $^3J_{HH}$ = 7.6 Hz, 2 H, bdt), 7.34 (d, $^3J_{HH}$ = 7.6 Hz, 2 H, bdt), 7.43–7.61 (m, 6 H, Ph), 7.79–7.95 (m, 4 H, Ph). **^{31}P{^{1}H} NMR** ([D$_6$]DMSO): δ = 57.6 (s, $^1J_{P,^{195}Pt}$ = 2892 Hz). (+)-**ESI-MS**: 896.04 [MNa$^+$]. $C_{38}H_{32}P_2PtS_4$ (873.95 g·mol^{-1}): calcd. C 52.23 H 3.69 S 14.67 %, found C 52.41 H 3.91 S 14.30 %. Single crystals suitable for an X-ray diffraction study were obtained by recrystallization from DMF.

Complex 5: Au(PPh$_3$)Cl (99 mg, 0.20 mmol) and NEt$_3$ 50 µL, 0.40 mmol) were added to a suspension of **2** (80 mg, 0.10 mmol) in CHCl$_3$ (5 mL). A clear solution formed immediately. After stirring overnight, MeOH was added until a golden orange precipitate formed. The solids were collected by filtration and washed with MeOH and Et$_2$O (3 × 10 mL each). The crude product was recrystallized by layering a saturated solution in CHCl$_3$ with ethyl acetate. Yield 115 mg (80 %). **^{1}H NMR** (CDCl$_3$): δ = 3.48 (m, 1 H, CH$_2$), 3.59 (d, $^2J_{PH}$ = 12.0 Hz, 2 H, CH$_2$), 4.05 (m, 1 H, CH$_2$), 6.12 (d, $^3J_{HH}$ = 7.7 Hz, 1 H, bdt), 6.35 (dd, $^3J_{HH}$ = 7.7, $^3J_{HH}$ = 7.6 Hz, 1 H, bdt), 6.88–7.09 (m, 4 H, bdt), 7.09–7.41 (m, 22 H, Ph), 7.43–7.67 (m, 10 H, Ph), 8.03 (br., 1 H, Ph), 8.22 (br., 2 H, Ph). **^{31}P{^{1}H} NMR** (CDCl$_3$): δ = 64.5 (d, J_{PP} = 7.7 Hz), 36.1 (s), 19.1 (d, J_{PP} = 7.7 Hz). $C_{56}H_{45}Au_2P_3PdS_4$·CHCl$_3$·C$_4$H$_7$O$_2$ (1439.5 g·mol^{-1}): calcd. C 46.73 H 3.15 S 8.91 %, found C 46.72 H 3.16 S 8.98 %.

Complex 6: Phosphane **2** (200 mg, 0.60 mmol) was dissolved in degassed MeCN (20 mL). KO*t*Bu (135 mg, 1.20 mmol) and [Pd(cod)Cl$_2$] (171 mg, 0.600 mmol) were added and the mixture agitated in an ultrasound bath until a red brown precipitate formed. The mixture was then stirred overnight. The solids formed were filtered off and the residue washed with MeCN (3 × 10 mL) and then re-dissolved in THF (20–30 mL). The clear solution was concentrated to one fourth of its original volume. Storage at –28 °C gave dark red crystals that were washed with cold THF (5 mL) and Et$_2$O (3 × 5 mL) and then dried in vacuo. A second crop of crystals was obtained by storing the combined mother liquid and wash solvents. Yield 139 mg (48 %). **^{1}H NMR** (CD$_2$Cl$_2$): δ = 3.62–3.84 (m, 4 H, CH$_2$), 6.19 (d, $^3J_{HH}$ = 7.2 Hz, 2 H, bdt), 6.53 (dd, $^3J_{HH}$ = 7.9, $^3J_{HH}$ = 7.2 Hz, 2 H, bdt), 6.93 (d, $^3J_{HH}$ = 7.9 Hz, 2 H, bdt), 7.11–7.30 (m, 4 H, Ph), 7.31–7.46 (m, 6 H, Ph), 7.48–7.63 (m, 6 H, Ph), 7.76–7.92 (m, 4 H, Ph). **^{31}P{^{1}H} NMR** (CD$_2$Cl$_2$): δ = 57.3 (s). (+)-**ESI-MS**: 890.89 [MH$^+$]. $C_{38}H_{30}P_2Pd_2S_4$·C$_4$H$_8$O (961.79 g·mol^{-1}): calcd. C 52.45 H 3.98 S 13.33 %, found C 51.69, H 3.82, S 13.17 %.

Complex 7: A microwave reaction vessel (volume 30 mL) was charged with a solution of **2** (200 mg, 0.600 mmol) in THF/DMSO (95:5, 10 mL), [(cod)PdCl$_2$] (256 mg, 0.900 mmol) and NEt$_3$ (0.17 mL, 1.2 mmol). The vessel was closed and heated for 30 min to 180 °C in a microwave reactor. After the vessel had been allowed to cool down to ambient temperature, the orange precipitate formed was separated by filtration. Recrystallization from boiling DMSO (10 mL) afforded shining orange crystals that were washed with DMSO (5 mL) and acetone (3 × 10 mL) and dried in vacuo. Yield 247 mg (72 %). **^{1}H NMR** ([D$_6$]DMSO): δ = 2.50 (s, 6 H, DMSO), 3.86–4.08 (m, 4 H, CH$_2$), 6.47 (d, $^3J_{HH}$ = 7.4 Hz, 2 H, bdt), 6.81 (m, 6 H, Ph + bdt), 7.04–7.19 (m, 6 H, Ph), 7.31 (d, $^3J_{HH}$ = 8.0 Hz, 2 H, bdt), 7.64–7.79 (m, 6 H, Ph), 8.20–8.30 (m, 4 H, Ph). **^{31}P{^{1}H} NMR** ([D$_6$]DMSO): δ = 71.9 (s). $C_{38}H_{30}P_2Pd_3S_4$·C$_2$H$_6$OS (1145.13 g·mol^{-1}): calcd. C 41.96 H 3.17 S 14.00 %, found C 41.83 H 3.16 S 13.95 %.

Complex 8: The synthesis was carried out as described for **6** using [NiCl$_2$(H$_2$O)$_6$] (143 mg, 0.600 mmol), except that CH$_2$Cl$_2$ rather than THF was used to re-dissolve the crude product for recrystallization. Yield 191 mg (68 %). **^{1}H NMR** (CD$_2$Cl$_2$): δ = 1.75 (m, 8 H, THF), 3.26 (br. d, $^2J_{HH}$ = 12.9 Hz, 2 H, CH$_2$), 3.44 (br. dd, $^2J_{PH}$ = 14.8, $^2J_{HH}$ = 12.9 Hz, 2 H, CH$_2$), 3.70 (m, 8 H, THF), 6.25 (d, $^3J_{HH}$ = 7.2 Hz, 2 H, bdt), 6.64 (dd, $^3J_{HH}$ = 8.0, $^3J_{HH}$ = 7.2 Hz, 2 H, bdt), 6.98 (d, $^3J_{HH}$ = 8.0 Hz, 2 H, bdt), 7.11–7.23 (m, 4 H, Ph), 7.24–7.40 (m, 6 H, Ph), 7.45–7.61 (m, 6 H, Ph), 7.95–8.09 (m, 4 H, Ph). **^{31}P{^{1}H} NMR** (CD$_2$Cl$_2$): δ = 51.9 (s). (+)-**ESI-MS**: 794.94 [MH$^+$], 816.93 [MNa$^+$]. $C_{38}H_{30}Ni_2P_2S_4$·2 C$_4$H$_8$O (936.06 g·mol^{-1}): calcd. C 58.88 H 4.94 S 13.67 %, found C 58.68 H 4.90 S 13.64 %.

Complex 9: Agitation of a suspension of [PdCl$_2$(cod)] (168 mg, 0.587 mmol) and **2** (150 mg, 0.590 mmol) in pyridine (10 mL) for 1 h in an ultrasound bath produced a dark red solution which was stirred for 4 days at 50 °C. Addition of MeO*t*Bu (28 mL) produced a solid material that was filtered off and washed with MeO*t*Bu (10 mL) and degassed MeOH (3 × 10 mL). A ^{31}P NMR spectrum recorded after dissolution in THF revealed the presence of a mixture of **3** and **6** (ca. 2:1). This solution was heated in a microwave reactor to 170 °C for 15 min. Bright red prisms of **9** formed as the solution was cooled down to ambient temperature were separated by manual picking and recrystallized from CH$_2$Cl$_2$ (no yield determined). A ^{31}P NMR spectroscopic assay revealed that formation of **9** had occurred at the expense of **3**. **^{1}H NMR** (CD$_2$Cl$_2$): δ = 1.82 (m, 4 H, THF), 3.68 (m, 4 H, THF), 3.90 (d, $^2J_{PH}$ = 10.3 Hz, 6 H, CH$_2$), 5.33 (s, 2 H, CH$_2$Cl$_2$), 6.36 (br. d, $^3J_{HH}$ = 7.2 Hz, 3 H, bdt), 6.57 (ddd, $^3J_{HH}$ = 7.9, $^3J_{HH}$ = 7.2, J_{PH} = 0.5 Hz, 3 H, bdt), 6.81 (ddd, $^3J_{HH}$ = 7.9, $^4J_{HH}$ = $^4J_{PH}$ = 1.5 Hz, 3 H, bdt), 7.36 (m, 12 H, Ph), 7.44 (m, 6 H, Ph), 7.60 (m, 12 H, Ph). **^{31}P{^{1}H} NMR** (CD$_2$Cl$_2$): δ = 52.1 (s). $C_{57}H_{45}Pd_3P_3S_6$·CH$_2$Cl$_2$·THF (1491.58 g·mol^{-1}): calcd. C 49.92 H 3.74 S 12.90 %, found C 50.29 H 3.81 S 12.67 %.

Computational Studies: Density functional theory (DFT) calculations were performed with the ORCA program package[17] using the B3LYP functional[18] with the def2-TZVP and Weigend J auxiliary basis set[19] and the RIJCOSX approximation. Dispersion corrections were applied using Grimme's D3BJ formalism.[20] Geometry optimization was done with the TightSCF convergence option (1.0e-7 a.u.), and solvation in CH$_2$Cl$_2$ was modeled using the CPCM solvation model.[21] Geometry optimization of [Ni$_2$(pbdt)$_2$] (**8**) was carried out at the restricted Kohn–Sham DFT level starting from the experimental geometry. Calculations on [Ni$_2$(pbdt)$_2$]^q (q = 1+/1/2–) were performed at the unrestricted Kohn–Sham DFT level by removing/adding 1e$^-$ or 2e$^-$ with the same basis set and functionals.

Supporting Information (see footnote on the first page of this article): Crystallographic data for **4**–**9**, graphical representations of the molecular structures of complexes **6** and **8**, cyclic voltammetry data, computational results.

Acknowledgements

We thank *Barbara Förtsch* (Institut für Anorganische Chemie) for measuring elemental analyses and *Martin Trinkner* and *Dr. Wolfgang Frey* (both from Institut für Organische Chemie) for measuring ESI mass spectra and collecting X-ray data sets. M.R.R. gratefully acknowledges support by the State of Baden-Württemberg through bwHPC and the German Research Foundation (DFG) through grant no. INST 40/467–1 FUGG for access to the Justus cluster. Open access funding enabled and organized by Projekt DEAL.

Keywords: P ligands; S ligands; Bridging ligands; Group-10 metals; Microwave assisted synthesis

References

[1] Selected reviews: a) T. Shiga, G. N. Newton, H. Oshio, *Dalton Trans.* **2018**, *47*, 7384–7394; b) B. R. Manzano, F. A. Jalon, M. C. Carrion, G. Dura, *Eur. J. Inorg. Chem.* **2016**, 2272–2295; c) P. Thanasekaran, C.-C. Lee, K.-L. Lu, *Acc. Chem. Res.* **2012**, *45*, 1403–1418; d) A. J. Boydston, C. W. Bielawski, *Dalton Trans.* **2006**, 4073–4077.

[2] Selected reviews: a) N. C. Burtch, K. S. Walton, *Acc. Chem. Res.* **2015**, *48*, 2850–2857; b) Z. Yin, Y.-L. Zhou, M.-H. Zeng, M. Kurmoo, *Dalton Trans.* **2015**, *44*, 5258–5275; c) M. Higuchi, *J. Mater. Chem. C* **2014**, *2*, 9331–9341; d) N. Ahmad, A. H. Chughtai, H. A. Younus, F. Verpoort, *Coord. Chem. Rev.* **2014**, *280*, 1–27; e) G. Schwarz, I. Hasslauer, D. G. Kurth, *Adv. Colloid Interf. Sci.* **2014**, *207*, 107–120.

[3] S. Chikkali, D. Gudat, *Eur. J. Inorg. Chem.* **2006**, 3005–3009.

[4] S. H. Schlindwein, K. Bader, C. Sibold, W. Frey, P. Neugebauer, M. Orlita, J. van Slageren, D. Gudat, *Inorg. Chem.* **2016**, *55*, 6186–6194.

[5] a) S. H. Chikkali, D. Gudat, F. Lissner, M. Niemeyer, T. Schleid, M. Nieger, *Chem. Eur. J.* **2009**, *15*, 482–491; b) G. Bauer, Z. Benkő, J. Nuss, M. Nieger, D. Gudat, *Chem. Eur. J.* **2010**, *16*, 12091–12095; c) G. Bauer, M. Nieger, D. Förster, D. Gudat, *Z. Anorg. Allg. Chem.* **2014**, *640*, 325–333; d) G. Bauer, M. Nieger, D. Gudat, *Dalton Trans.* **2014**, *43*, 8911–8920; e) S. H. Schlindwein, S. Hänisch, M. Nieger, D. Gudat, *Eur. J. Inorg. Chem.* **2017**, 3834–3842.

[6] S. H. Schlindwein, PhD Thesis, Stuttgart **2018**.

[7] Median and standard deviation returned by a query in the CSD for P–Pd distances in tetra-coordinate palladium complexes.

[8] See for example: a) H. Schmidbaur, *Gold Bull.* **1990**, *23*, 11–23; b) H. Schmidbaur, A. Schier, *Chem. Soc. Rev.* **2012**, *41*, 370–412, and references therein.

[9] R. Cao, Z. Huang, X. Lei, B. Kang, M. Hong, H. Liu, *Chin. J. Chem.* **1992**, *10*, 227–232.

[10] See e.g.: a) Y. Nakamura, T. Matsumoto, Y. Sakazume, J. Murata, H.-C. Chang, *Chem. Eur. J.* **2018**, *24*, 7398–7409; b) A. Kochem, T. Weyhermüller, F. Neese, M. van Gastel, *Organometallics* **2015**, *34*, 995–1000; c) K. Ray, T. Weyhermüller, F. Neese, K. Wieghardt, *Inorg. Chem.* **2005**, *44*, 5345–5360.

[11] L. Gan, T. L. Groy, P. Tarakeshwar, S. K. S. Mazinani, J. Shearer, V. Mujica, A. K. Jones, *J. Am. Chem. Soc.* **2015**, *137*, 1109–1115.

[12] A. Mondragón-Díaz, E. Robles-Marín, B. A. Murueta-Cruz, J. C. Aquite, P. R. Martínez-Alanis, M. Flores-Alamo, G. Aullón, L. N. Benítez, I. Castillo, *Chem. Asian J.* **2019**, *14*, 3301–3312.

[13] R. H. Harris, E. D. Becher, S. M. Cabral de Menezes, R. Goodfellow, P. Granger, *Concepts Magn. Reson.* **2002**, *14*, 326–346.

[14] G. M. Sheldrick, *Acta Crystallogr., Sect. A* **2008**, *64*, 112–122.

[15] G. M. Sheldrick, *Acta Crystallogr., Sect. C* **2015**, *71*, 3–8.

[16] A. L. Spek, *Acta Crystallogr., Sect. C* **2015**, *71*, 9–18.

[17] F. Neese, *WIREs Comput. Mol. Sci.* **2012**, *2*, 73–78.

[18] P. J. Stephens, F. J. Devlin, C. F. Chabalowski, M. J. Frisch, *J. Phys. Chem.* **1994**, *98*, 11623–11627.

[19] a) F. Weigend, R. Ahlrichs, *Phys. Chem. Chem. Phys.* **2005**, *7*, 3297–3305; b) F. Weigend, M. Häser, H. Patzelt, R. Ahlrichs, *Chem. Phys. Lett.* **1998**, *294*, 143–152.

[20] S. Grimme, J. Antony, S. Ehrlich, H. Krieg, *J. Chem. Phys.* **2010**, *132*, 1.

[21] Y. Takano, K. N. Houk, *J. Chem. Theory Comput.* **2005**, *1*, 70–77.

Received: December 23, 2019
Published Online: February 20, 2020

